2 FINAL REPORT ON

"INVESTIGATION OF A MULTIPLE QUANTUM WELL ELEMENT FOR OPTICAL MODULATION AND OPTICAL SWITCHING"

Scientific Authority: Dr. Kenneth O. Hill
CRC, Ottawa

Principal Investigator: Dr. Michael Cada
EE-TUNS, Halifax

Collaborators:
B.P. Keyworth - TUNS, Halifax
J.M. Glinski - BNR, Ottawa
C. Rolland - BNR, Ottawa
A.J. SpringThorpe - BNR, Ottawa
P. Mandeville - BNR, Ottawa
R. Normandin - NRC, Ottawa
R. Soref - RADC, Hanscom, USA

Table of Contents

Optical Switching in a GaAs-based Multiple Quantum Well Nonlinear Directional Coupler

Abstract

The rapidly developing fields of optical communications and optical computing have stimulated extensive research toward integrated optoelectronic devices. One of the most promising developments to come out of this effort was the invention of a new class of "man-made" materials called multiple quantum wells (MQW's). These multilayered structures exhibit improved performance in electrooptical as well as all-optical switching functions and offer a great potential for future device applications. However, since the market for these devices still relies heavily on conventional electronic components, the application of optical systems under electronic control seems much more near term. This report therefore concentrates on the electric-field dependent switching in a nonlinear MQW directional coupler.

1. Introduction

The need to transmit and/or process information more reliably and at an ever increasing rate has yielded impressive advancements in lightwave communications. However, the area of integrated optoelectronics is still in a fairly immature state. We therefore find ourselves in a position where the means to transmit optical information is in place but the high speed processing remains a problem. Ideally, ultra-fast, all-optical devices are required in order to completely eliminate the slower electronic components. These devices should also be capable of monolithic integration with optical sources and detectors. More realistically, at least for short term applications, there is a demand for fast electrooptic devices which may be integrated with high speed electronics in addition to sources and detectors.

In recent years, Gallium Arsenide (GaAs) and Indium Phosphide (InP) integrated circuits have emerged capable of data rates approaching 10 GHz [1]. This figure is very close to that available with state-of-the-art GaAlAs or GaInAsP laserdiodes and photodetectors [2,3]. Also, since they are both compound semiconductors, GaAs (InP) can be lattice-matched to GaAlAs (GaInAsP), which allows monolithic integration of sources, detectors, and electronics. It is clear therefore, that to fully exploit the best technologies available today we require new optoelectronic components which employ the same semiconductor compounds.

1.1 Multiple Quantum Wells

Multiple quantum well (MQW) structures formed by alternating ultrathin layers of two semiconductors with different band-gap energies have demonstrated completely new characteristics not found in the bulk materials [4-8]. The improved optical nonlinearity and electrooptic effect attained with these new composite layers show great promise for the "missing link" in optical systems. MQW's are well suited for this application since the research work to date has concentrated on GaAs/AlGaAs and InP/GaInAsP quantum wells.

Since they were first proposed by Esaki and Tsu in 1969 [9], MQW's (and superlattices) have received much attention. However, the implementation of these structures was delayed until the growth technology became available in the 1980's. Today they are grown by either molecular beam epitaxy (MBE) or

metal-organic-chemical-vapor deposition (MOCVD) technique. Most of the research work done to date on MQW structures has concentrated on those consisting of alternating layers of GaAs and AlGaAs. As with all other MQW's, the layers are composed of semiconductors with two different band gap energies. The typical band structure of a multiple quantum well is shown in Figure 1.

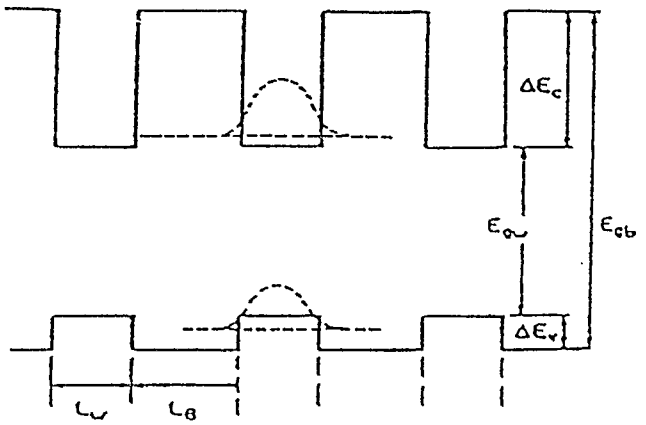

Figure 1. Band structure of a multiple quantum well.

From this figure it can be seen that the lower band gap energy of the GaAs layers results in periodically spaced potential wells surrounded by AlGaAs barriers. Photo-excited electron-hole pairs are confined to the potential wells due to the differences in conduction-band and valence-band energies. This confinement perturbs the band structure of the wells and creates a finite number of allowed subbands for the electrons and holes. In their low energy states the electron-hole pairs are bound together by Coulomb forces and are referred to as excitons. It is the presence of these states that makes MQW materials so attractive.

At extremely low temperatures, excitonic effects can be observed in both MQW's and their bulk semiconductors. This is noted by one or two resonance peaks near the absorption edge of the material. However, at room temperature the weakly bound excitons in the bulk semiconductors are ionized by interaction with phonons and the absorption peaks disappear. This is not the case in MQW's

because the quantum confinement actually flattens the excitons, increasing the Coulomb attraction and preventing the electron-hole pairs from being torn apart. The low temperature absorption spectra of bulk GaAs and a GaAs/AlGaAs MQW are compared in Figure 2. The presence of both a heavy hole and a light hole in the valence band of the MQW results in the observation of two resonance peaks in its absorption spectrum, with the strength of each peak being proportional to the spacing between the electrons and holes.

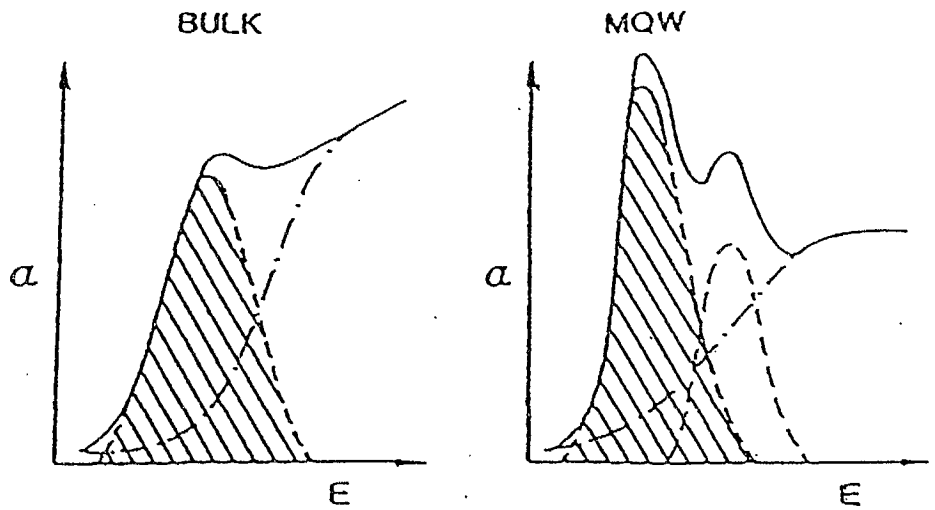

Figure 2. Absorption spectra of bulk GaAs and a GaAs/AlGaAs MQW.

The excitonic effects in MQW's disappear at high optical intensities as a result of screening of the Coulomb forces by free-carriers created either directly or through exciton ionization, or as a result of band filling. This leads to saturation of the optical nonlinearity in MQW's at intensities as low as 580 W/cm^2 near the absorption edge [5]. At saturation the exciton resonance peaks in the absorption spectrum disappear and the MQW behaves much like the bulk semiconductors. The change in absorption as optical intensity is increased can be related through the Kramers-Kronig relation to changes in the effective refractive index of the MQW layer [10].

Previous works have demonstrated that the absorption spectra of MQW's are also succeptable to electric field effects [7],[11-15]. This electric field dependency is referred to as the Quantum-Confined Stark Effect (QCSE) and is not present in the bulk materials. The mechanism involved in this effect is the pulling of the electrons and holes to opposite sides of the well thereby reducing the energy of an electron-hole pair. The name is derived from a similar phenomenon in Hydrogen atoms known as the Stark Effect.

1.2 The Quantum-Confined Stark Effect

Due to the quantum-confined Stark effect the exciton absorption peaks are shifted to lower energies (longer wavelengths) when an external electric field is applied perpendicular to the quantum well layers. There is also some degradation of the resonance peaks associated with this shift since the excitons are more weakly bound and therefore ionize more readily. However, the peaks may be clearly resolved in the absorption spectra for wavelength shifts of several nanometers [7]. In bulk semiconductors the weakly bound excitons present at low temperatures are torn apart by the applied field and the absorption peak disappears leaving only a slight shift and spreading of the absorption edge associated with the Franz-Keldysh effect [16]. In quantum wells the confinement of the exciton prevents the field ionization and the peaks are preserved. Shifts of 40 meV (24 nm) have been observed in the absorption spectra at field strengths of 22 V/μm.

These shifts in the absorption spectrum produce large changes in the effective refractive index of the MQW layer as illustrated in figure 3 [17]. Here the change in real refractive index n near the absorption edge is plotted along with the extinction coefficient k for applied electric fields of 0 and 10 V/μm. The extinction coefficient is directly related to absorption and it can be seen that at a field strength of 10 V/μm a shift of approximately 11 nm is achieved. However, if the wavelength of operation is chosen to be 848 nm, which is about 2 nm above the resonance peak in this case, the absorption remains unchanged when alternating the electric field between the two values indicated. In comparison, a

change in refractive index of approximately 0.1 occurs at the same wavelength. This is very attractive for applications that require electrorefraction without electroabsorption, *e.g.* low insertion loss electrooptic switches.

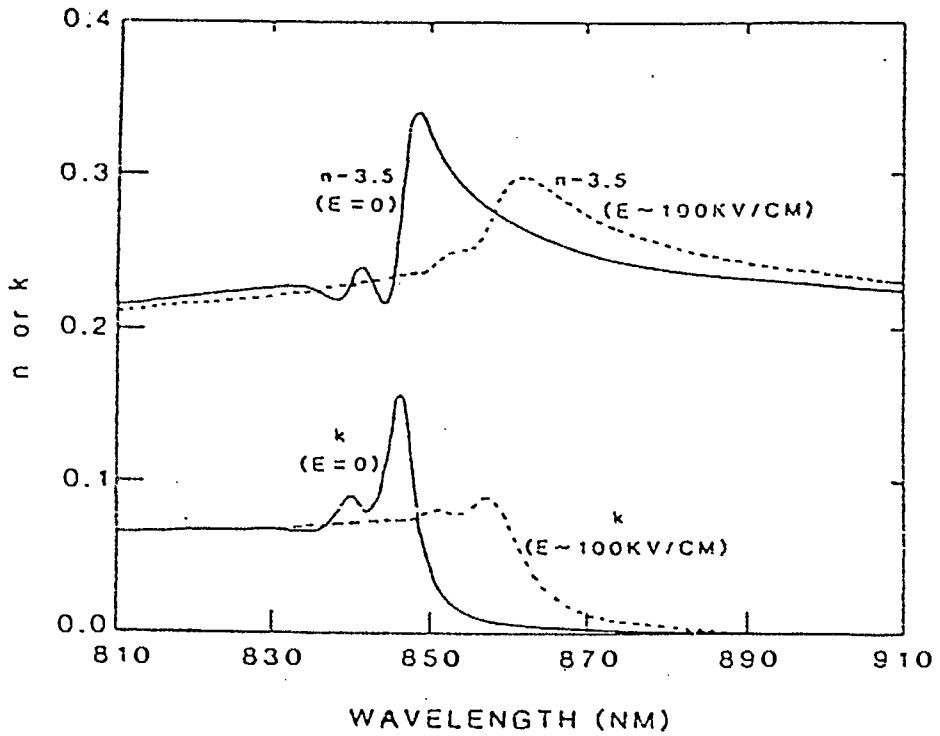

Figure 3. Quantum-confined Stark effect in a GaAs/AlGaAs MQW.

1.3 Applications of MQW's

Since their introduction, multiple quantum well materials have been incorporated into a wide variety of device applications [18-25]. These include MQW-based lasers, mode-lockers, optical modulators, all-optical switches, electro-optic switches, optical logic gates, and bistable devices. There are a variety of mechanisms which may be employed in such devices including the nonlinear, intensity-dependent refractive index or absorption changes in MQW structures, and electroabsorption or electrorefraction associated with the QCSE.

The devices of most relevance to the work described in this report are the all-optical and electro-optic switches. The majority of these are based on the directional coupler in which two matched waveguides are placed in close enough proximity as to allow a periodic transfer of optical power from one waveguide to the other. The critical length L_c required to obtain a complete transfer depends on the physical dimensions of the structure and on the refractive indices of the waveguides and the center coupling medium. Therefore, if, for example, the refractive index of the coupling medium can be externally controlled, the critical coupling length can be modified which produces a switching effect.

2. The Nonlinear Directional Coupler

2.1 Background

The nonlinear coherent coupler (NLCC) was first described by Jensen in 1980 [26]. This device is simply a directional coupler with a nonlinear, Kerr-type material used in both coupled waveguides. In this structure the refractive index of the waveguides varies with the intensity of the guided light thereby producing all-optical switching. A variation of this design which used a multiple quantum well as the nonlinear material was demonstrated first by Li Kam Wa *et al.* in 1985 [23]. Their structure employed an MQW layer for the waveguides and the coupling layer. This was achieved by depositing two gold strips on an MQW substrate which condensed during cooling to form strain-induced waveguides. A transfer was obtained from a complete crossed-over state at low optical powers to less than 50 percent cross-coupled at 2 mW with a sample length of 1.7 mm.

The design for a MQW-coupled nonlinear directional coupler, where only the coupling medium properties can be controlled, with low-loss linear waveguides was first proposed by Cada *et al.* in 1986 [24] and demonstrated experimentally in 1988 [27]. The theoretical analysis of this first semiconductor ΔK switch has been presented elsewhere [28-30] and will not be repeated here. This analysis predicted that an abrupt transfer of optical energy will occur at launched optical powers near the critical value P_c. At power levels below this value the coupler will behave like a linear device with a periodic transfer of power. At

powers above P_c a complete transfer of power will no longer occur and the waveguides will become effectively uncoupled thus driving the output into a complete straight-through condition.

The basic structure under study here is illustrated in Figure 4. Two slightly different samples were actually fabricated and tested.

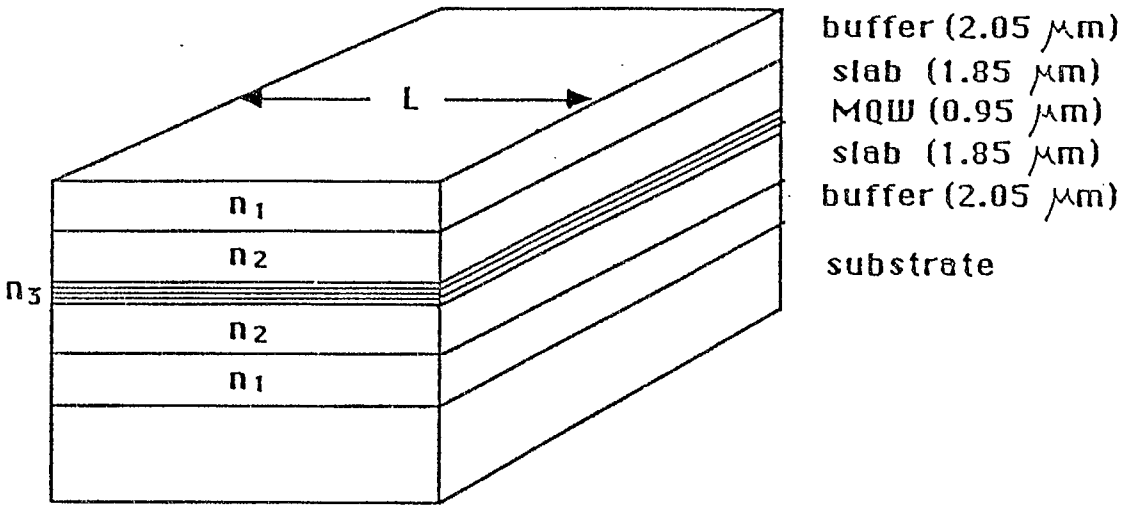

Figure 4. MQW-coupled, nonlinear waveguide switching element.

The coupling element is composed of two $Al_{.18}Ga_{.82}As$ planar waveguides of 1.85-μm-thickness, coupled through a 0.948-μm-thick MQW layer. The structure is buffered on both sides by 2-μm layers of $Al_{.72}Ga_{.28}As$. In the first samples, referred to as sample design 1, the MQW layer consists of 30 periods of alternating GaAs and $Al_{.33}Ga_{.67}As$ layers with well and barrier widths of 10.6nm and 21nm, respectively. In sample design 2 the MQW layer is slightly different. Here the well widths alternate between 10.6 nm and 8 nm with a constant barrier width of

21 nm bordering each well. The samples were fabricated by Molecular Beam Epitaxy (MBE) technique and were characterized using photoluminescence. This work was done by collaborators at Bell-Northern Research Ltd. Photoluminescence spectra revealed an exciton resonance peak at a wavelength of 848.6 nm in both sample designs and an additional peak at 837 nm in sample design 2, as shown in Figure 5.

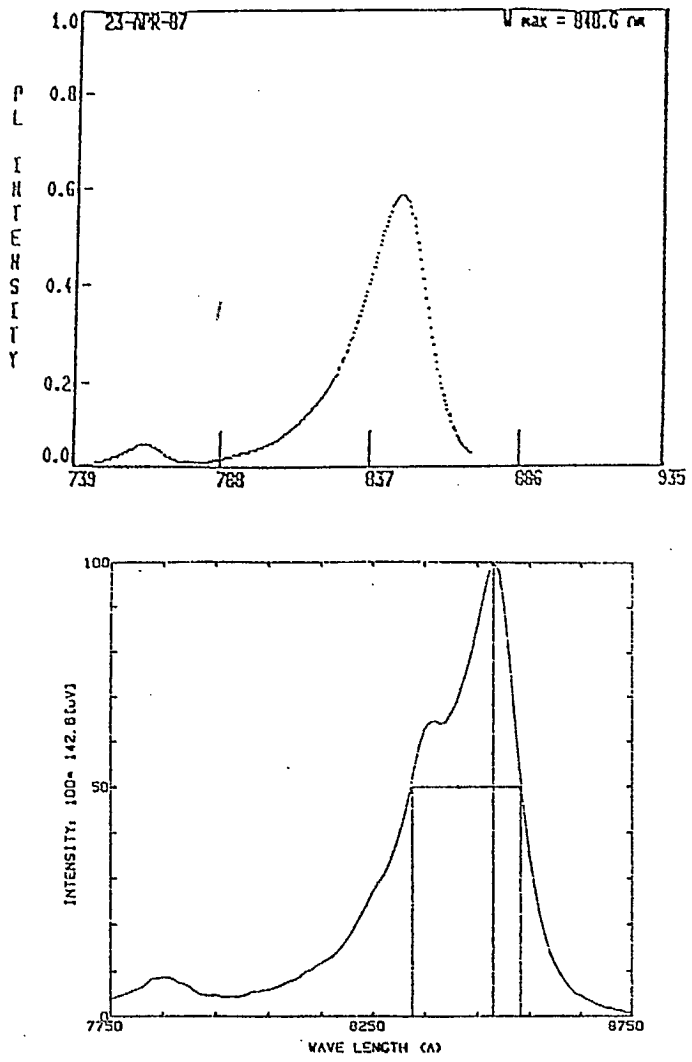

Figure 5. Photoluminescence spectra.
Top - Design #1, Bottom - Design #2

An important novel feature of this design is that for practical purposes the waveguide slabs may be considered linear and lossless. This is achieved by shifting the absorption edge of the waveguide material to higher energies by employing AlGaAs with a low aluminum content. The insertion losses of the device can therefore be attributed only to reflections at the cleaved end face and absorption in the MQW as light is coupled between the guides. The reduced losses allow the coupler to be operated at wavelengths closer to the excitonic absorption edge where the nonlinear effects are very strong.

2.2 Experimental Results.

The experimental arrangement used in testing the NLCC is shown in Figure 6. In order to provide a tunable light source, a CW argon laser is used as a pump beam for a Styryl-9 dye laser which emits in the near infrared region. This provides a vertically polarized source which is tunable over a 150-nm range of wavelengths, centered at 840nm. Remote control of the output power is provided by a dye laser stabilizer which clamps the output to within 2 percent of the set value. A variable beamsplitter was used to provide a sample beam for wavelength monitoring using a wavemeter.

Further control of the optical power is achieved with an acousto-optic modulator. The 2-mm-diameter beam is then focused to a spot size of approximately 1.5 micrometers at the input face of the coupler using a 60X microscope objective lens. A TE mode was selectively launched into one of the two waveguides by end-fire coupling the beam to a vertically mounted sample. In order to insure alignment of the incident polarization vector with the plane of the waveguides (and hence eliminate TM modes), a polarization rotating plate was placed before the input lens.

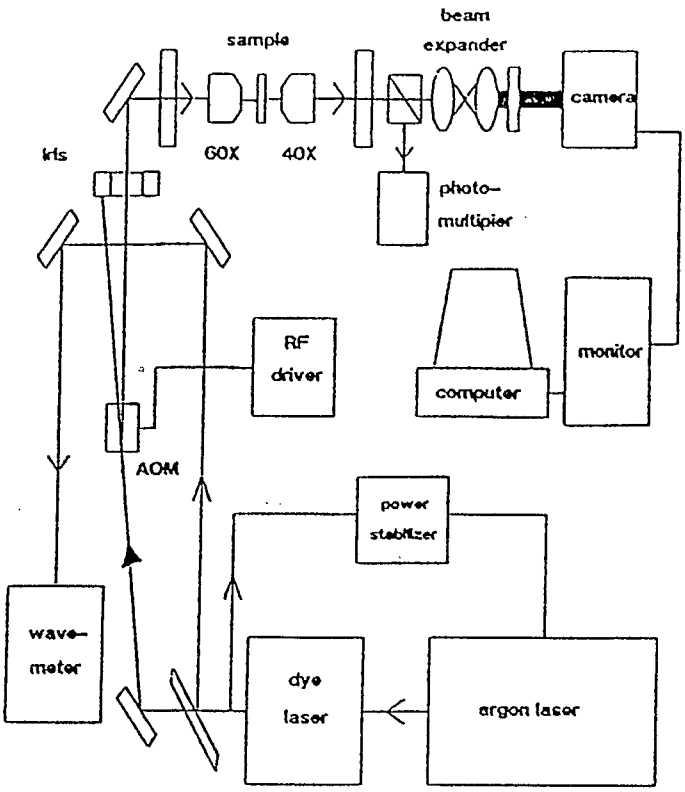

Figure 6. Experimental setup.

Since planar slabs are employed in the coupling device, the coupled light is allowed to diverge in the plane of the waveguides due to the lack of lateral confinement. Therefore, as the light propagates through the sample it is confined in one direction due to the waveguiding effect while it is allowed to diverge at an angle of 5.3° in the other direction to form a beam of approximately 50 μm width at the output of a 250-μm-long waveguide. Although this effect was not considered in the original analysis, the results were still in reasonably good agreement with experimental values.

At the output face of the coupler, a 40X objective lens was used in conjunction with a 12X beam expander to image the output from the sample onto the input aperture of an infrared camera. For long sample lengths, some of the light from the waveguides was outside the camera's field of view due to the divergence mentioned above. However, this was of no consequence to our results since we were only interested in the intensity distribution across the two waveguides which

are only a few micrometers wide. A second variable beamsplitter was placed in front of the camera in order to prevent saturation of the video display at higher output intensities.

The video output from the camera was connected to a high resolution monitor and to a personal computer. The computer was equipped with an image processing board which allowed the output image of the waveguides to be digitized and stored for later analysis. The digitized image has a resolution of 256 x 192 pixels which are stored as one of 256 grey levels. The intensity distribution across the two waveguides can then be readily obtained by scanning the pixel values across one line of the screen. In order to reduce the background scattered light, several lines can be averaged down the screen since the waveguides appear as two wide vertical lines which extend from the top to the bottom of the monitor.

2.3 All-Optical Switching.

From the calculations done using available experimental data, it followed that the coupling length required for a full intensity-dependent transfer of power was approximately 160 μm for sample design 1. The output intensity distribution at two values of incident optical power is shown in figure 7 for a sample length of 127 μm. The wavelength of operation is 850.5 nm which is about 2 nm above the heavy-hole exciton resonance peak. The incident beam is coupled into the bottom waveguide as indicated by the arrow at the bottom, left side of the plot. In the low power case, shown as a solid curve, the incident power of 10 μW produces an almost complete cross-coupled condition with approximately 77 percent in the crossed waveguide. A transfer of output power towards the straight-through state begins to occur at powers near 1.0 mW, leading to a 25 percent cross-coupled condition at 9.3 mW of incident optical power as indicated by the dashed curve.

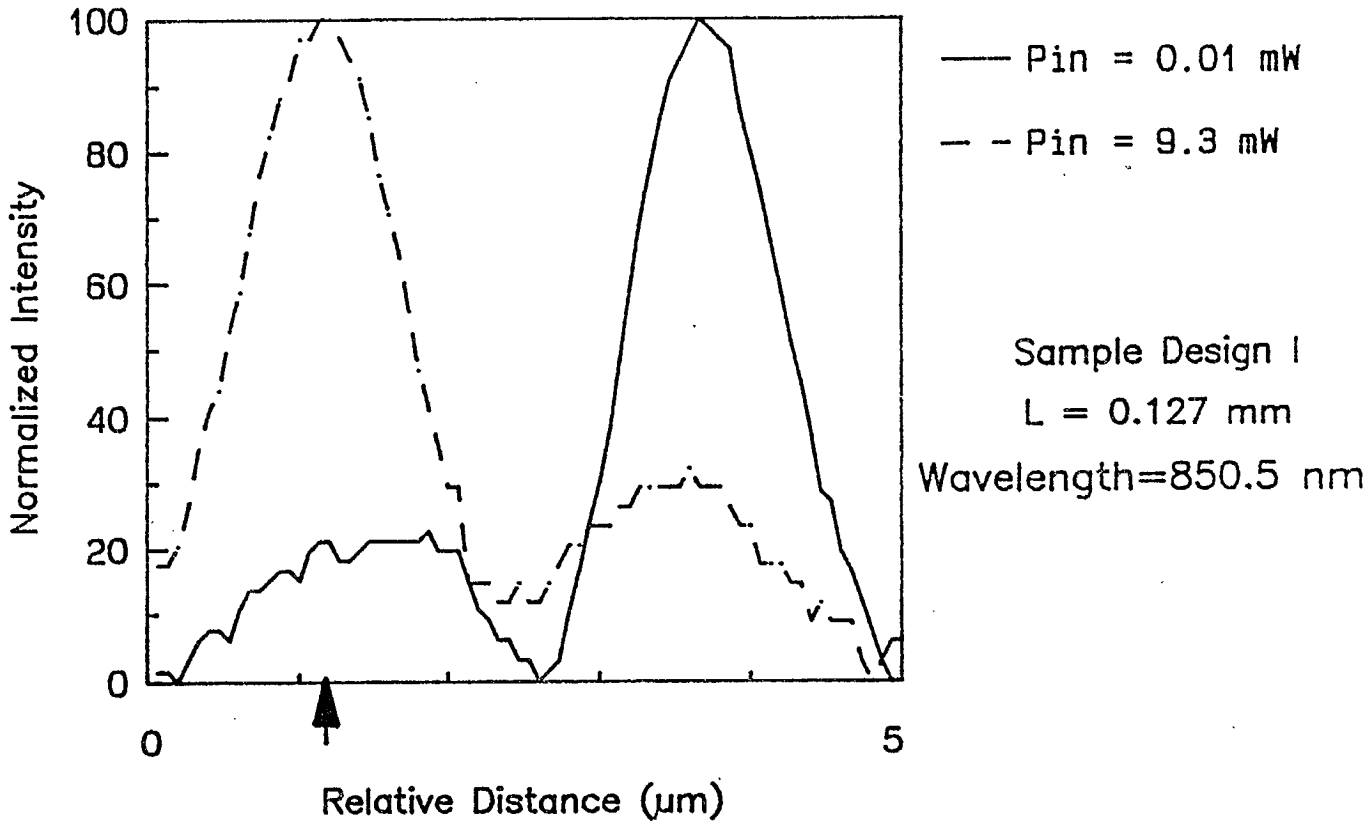

Figure 7. All-optical switching with a 127-μm sample.

A complete transfer of power is not achieved with the 127-μm sample for several reasons. The sample length is slightly less than the required full-transfer coupling length, therefore a full cross-coupled condition is not reached. The waveguides are not perfectly matched due to tolerances in the fabrication process which also prevents a complete cross-coupling. Finally, the focused spot at the input of the waveguides will saturate the nonlinearity at high powers and thus prevent a complete straight-through state.

A more efficient switching effect is expected for longer sample lengths near $2L_c$. This is verified by the curves in figure 8 which depict the intensity-dependent transfer for a sample length of 254 μm. In this case at low incident powers of approximately 50 μW the output distribution is mostly in the input waveguide. The incident energy is therefore transferred from the input waveguide to the crossed waveguide and back again. As the power is increased the output distribution is shifted towards the cross-coupled condition until, at an incident power of 1 mW, about 85 percent is in the crossed waveguide.

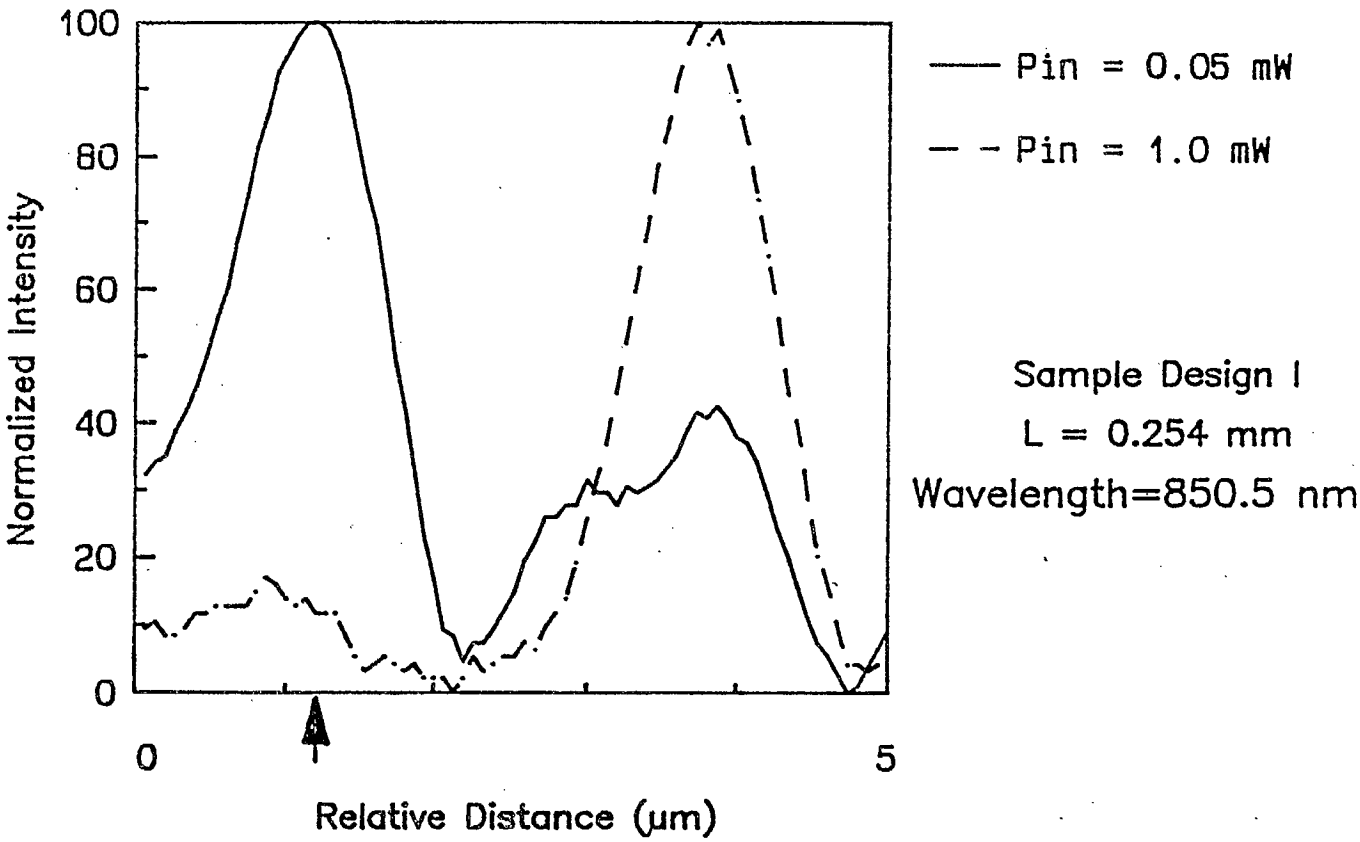

Figure 8. All-optical switching with a 254-μm sample.

This level of optical power required for intensity-dependent switching is well within the capabilities of commercially available semiconductor laserdiodes. A more detailed discussion of the all-optical switching obtained with sample design 1 can be found in [31].

3. Electrooptic Switching

3.1 Setup

The setup used for testing the electrooptic switching characteristics of the MQW-coupled nonlinear directional coupler was for the most part identical to that described earlier. The only difference being the addition of a means to apply an electric field to the samples. This field was applied perpendicular to the plane of the MQW layers by grounding the copper sample holder and connecting a positive electrode to the top of the coupler. This connection is made in one of two ways. In sample design 1, and in some of sample design 2, there is no provision for making an electrical connection. Therefore the electrode is simply placed over the top of the sample and a high bias voltage is applied. Large voltages are required since the field must penetrate the entire sample thickness of several hundred micrometers in order to achieve an appreciable strength in the MQW layer. Also the field is not distributed evenly over the sample but is instead localized under the tip of the electrode.

The latter problem was overcome in the second sample design by depositing a gold layer on top of the coupler and connecting a fine wire between the sample and a seperate metal contact. This allows easier placement of the positive electrode and produces a more even distribution of the electric field. Large bias voltages are still required however since we are using a relatively thick stack of intrinsic semiconducors and we require field strengths in the order of 1 V/μm for the quantum-confined Stark effect. This can be overcome in future devices by doping the substrate and perhaps the buffer layers so that the field is applied across a much shorter distance. This should reduce the required voltage by at least a factor of ten.

3.2 Sample Design 1

The setup used with the non-metalized samples provided limited success in electrooptic switching. The localized nature of the electric field made it difficult to achieve a substantial shift in the absorption spectrum of the MQW without exceeding the breakdown voltage at which arcing would occur. At lower voltages a change in absorption was observed but was not enough to produce a switching effect. After damaging several samples from the first design, as well as a microscope objective lens, electrooptic switching was achieved with a 406-μm-long sample at a wavelength of 851 nm. The output intensity distribution with and without an applied electric field is shown in figure 9.

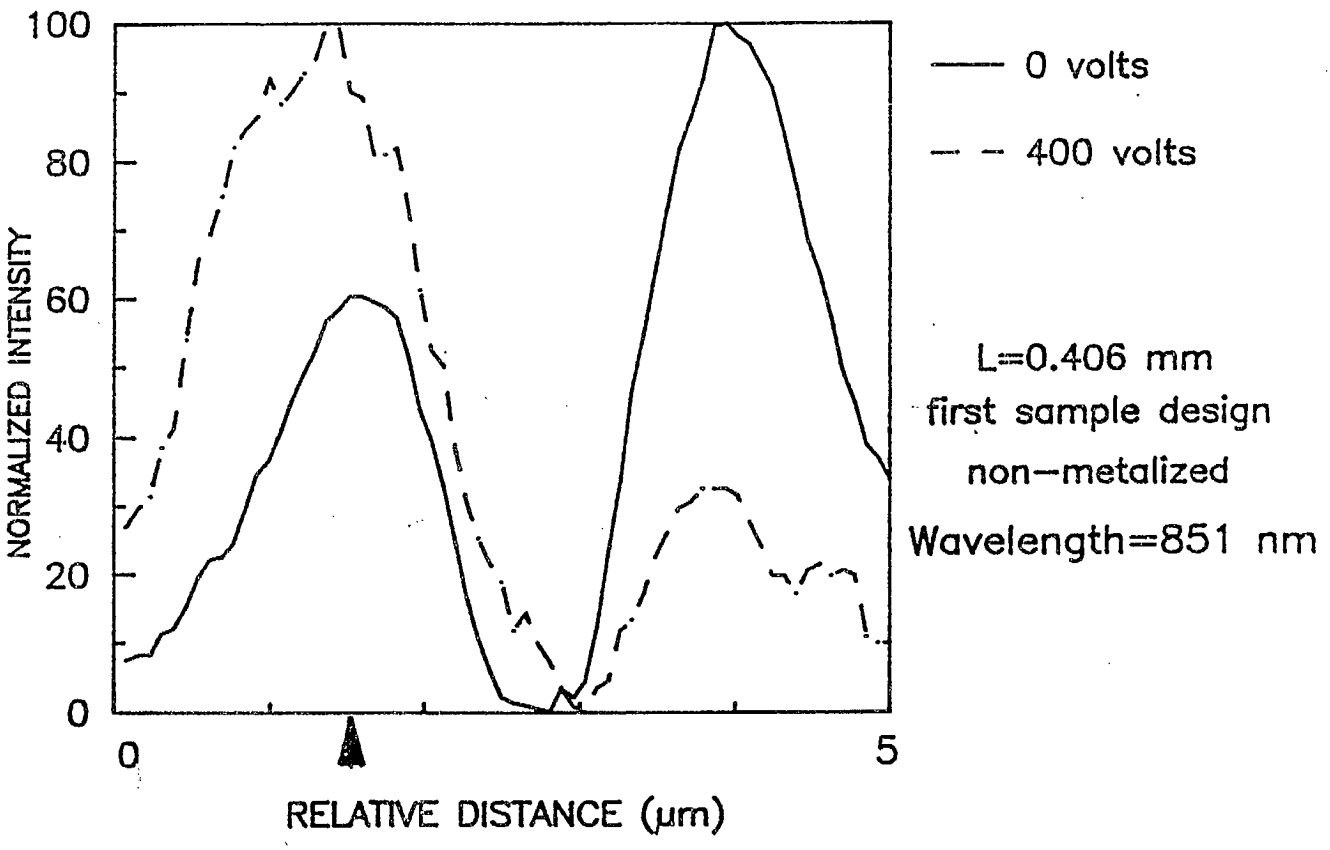

Figure 9. Electrooptic switching - Design #1.

The distribution is seen to shift from a partial cross-coupling with approximately 62 percent in the crossed waveguide at zero bias voltage to a mostly straight-through state at 400 volts. This voltage corresponds to an electric field strength of approximately 4 V/μm since the sample thickness is estimated at 100 μm. The switching effect obtained here is qualitatively similar to the all-optical switching obtained with the same sample, as reported in [32].

3.3 Sample Design 2

Figures 10 through 14 illustrate the electrooptic switching effects obtained with the second sample design. In figures 10 and 11, results are shown for a sample length of 800 μm at two different wavelengths. At 858 nm, shown by the first figure, a partial transfer is observed when coupling to the bottom waveguide. The distribution moves from one favoring the straight-through condition to one in which the crossed waveguide is stronger when a bias of 220 volts is applied across the 100 μm-thick sample. The required field strength is lower in this case since we are using a metalized sample which has a more uniform electric field as discussed earlier. The wavelength of operation here is shifted above the upper exciton absorption peak in order to reduce the losses in this relatively long sample. Unfortunately, these results are not duplicated if the incident beam is coupled into the top waveguide. This is due to a large asymmetry exhibited near the wavelength of 855 nm which is probably caused by a mismatch in the waveguides that becomes pronounced at this wavelength. When launching in the top waveguide the distibution remains unchanged when a field is applied and a strong cross-coupled condition is not reached.

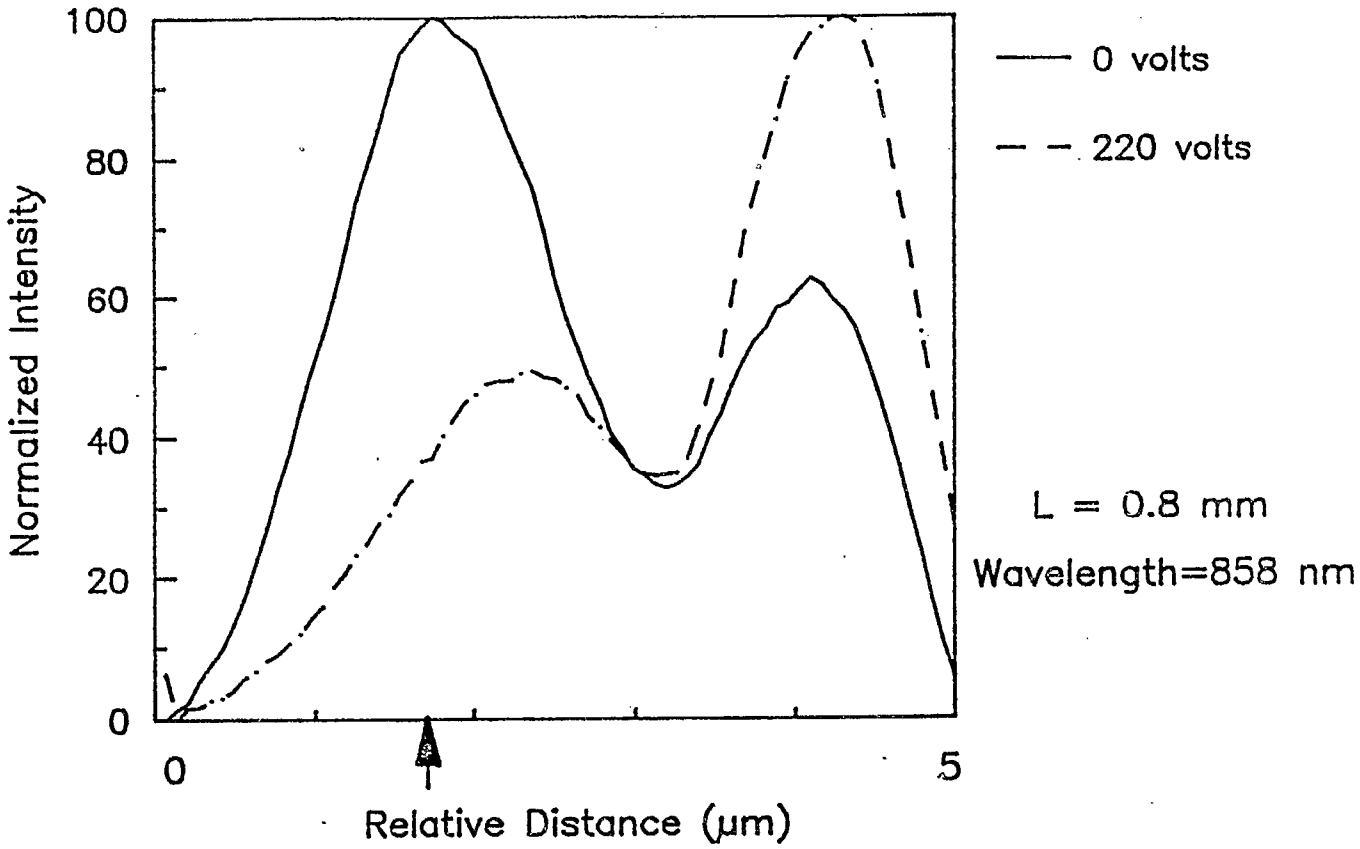

Figure 10. Electrooptic switching - Design #2, upper resonance.

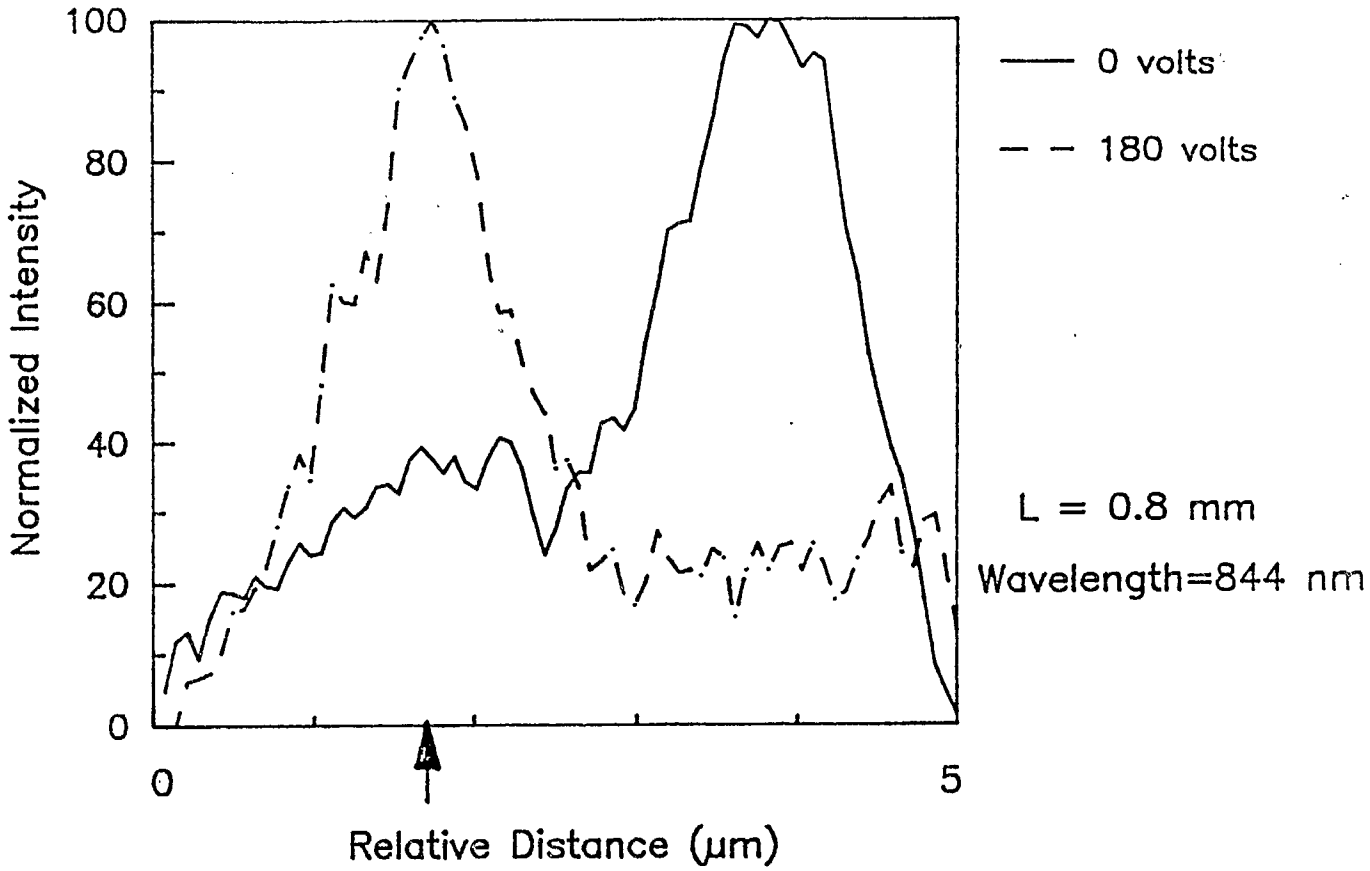

Figure 11. Electrooptic switching - Design #2, lower resonance.

The second case of electrooptic switching with this sample occurred at a wavelength of 844 nm as indicated in figure 11. Again the wavelength of operation was shifted away from the absorption peak; this time between the upper and lower exciton resonances. In this case the transfer of power is in the opposite direction to that at the longer wavelength. The distribution switches from a cross-coupled to a straight-through condition at a still lower bias voltage of 180 volts. The strong asymmetry experienced near 855 nm is not present at these shorter wavelengths so a similar effect can be achieved from the upper waveguide.

In order to verify that the mechanism involved in this switching effect is a shift in the absorption spectrum brought on by the quantum-confined Stark effect, the change in output distribution was observed as the wavelength of operation was manually shifted without any applied field. The wavelength dependency for

the 800-μm-long sample near 844 nm is shown for comparison in figure 12. We can see that a switching operation virtually identical to that depicted in figure 11 can be achieved by moving the wavelength of operation by approximately 2 nm toward shorter values. It therefore is justified to say that since the wavelength is fixed in the previous cases, the absorption spectrum of the MQW material was shifted by 2 nm towards longer wavelengths when the 180 volts of bias was applied. This corresponds to a shift of approximately 1.11 nm in the absorption spectrum per 1 V/μm of electric field, which compares very closely with results reported for similar MQW materials of 1.09 nm of shift per 1 V/μm [15].

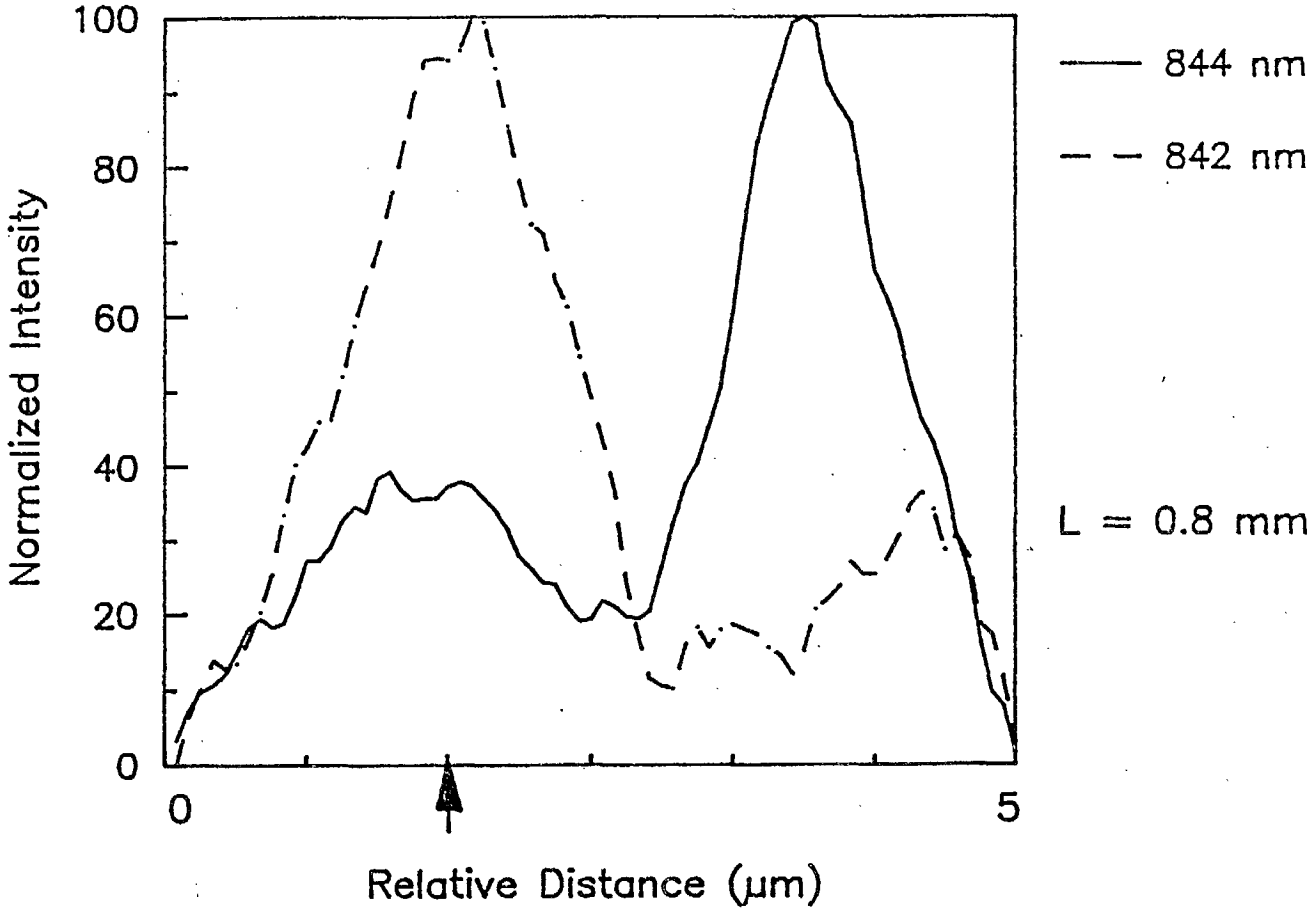

Figure 12. Wavelength dependent switching.

In order to operate the coupler at wavelengths closer to the exciton resonance peaks the sample length used must be kept small. Otherwise, the strongly attenuated output distribution cannot be detected by the infrared camera. Figures 13 and 14 reveal the electrooptic switching effects near the upper resonance wavelength for sample lengths of 600 μm and 500 μm, respectively. In figure 13, results are shown for a 600 μm metalized sample operated approximately 2.5 nm above the upper resonance peak where the refractive index of the MQW is near its maximum and a good transfer of power to the crossed waveguide is achieved. When a bias of 200 volts is applied, the spectrum is again shifted by approximately 2 nm towards the exciton peak and absorption increases. However, when operating at the middle of the resonance peak the refractive index of the MQW is lower compared to values slightly above the peak and the coupling is therefore reduced. This produces an electrooptic switching effect from the cross-coupled to the straight-through condition with field strengths of approximately 2 V/μm.

Figure 14 shows a similar effect for a sample length of 500 μm. In this case the gold layer was not present on the top of the sample but the required bias was the lowest achieved. This appears to contradict the assumption that placing an electrode over the top of the sample produces a non-uniform field and is a less efficient means of inducing electrooptic switching. However, it should be noted that the wavelength of operation here is slightly closer to the exciton resonance peak and in this region the refractive index of the MQW layer changes drastically with wavelength. It is therefore conceivable that the wavelength was better optimized at 851.2 nm so that a smaller wavelength shift was required for switching. Also, the 500 μm sample appears to be closer to the full-transfer coupling length at this wavelength since approximately 78 percent is cross-coupled from the bottom waveguide when no bias is applied. This distribution switches to a 35 percent crossed condition with a bias of 120 volts, corresponding to a low field strength of 1.2 V/μm.

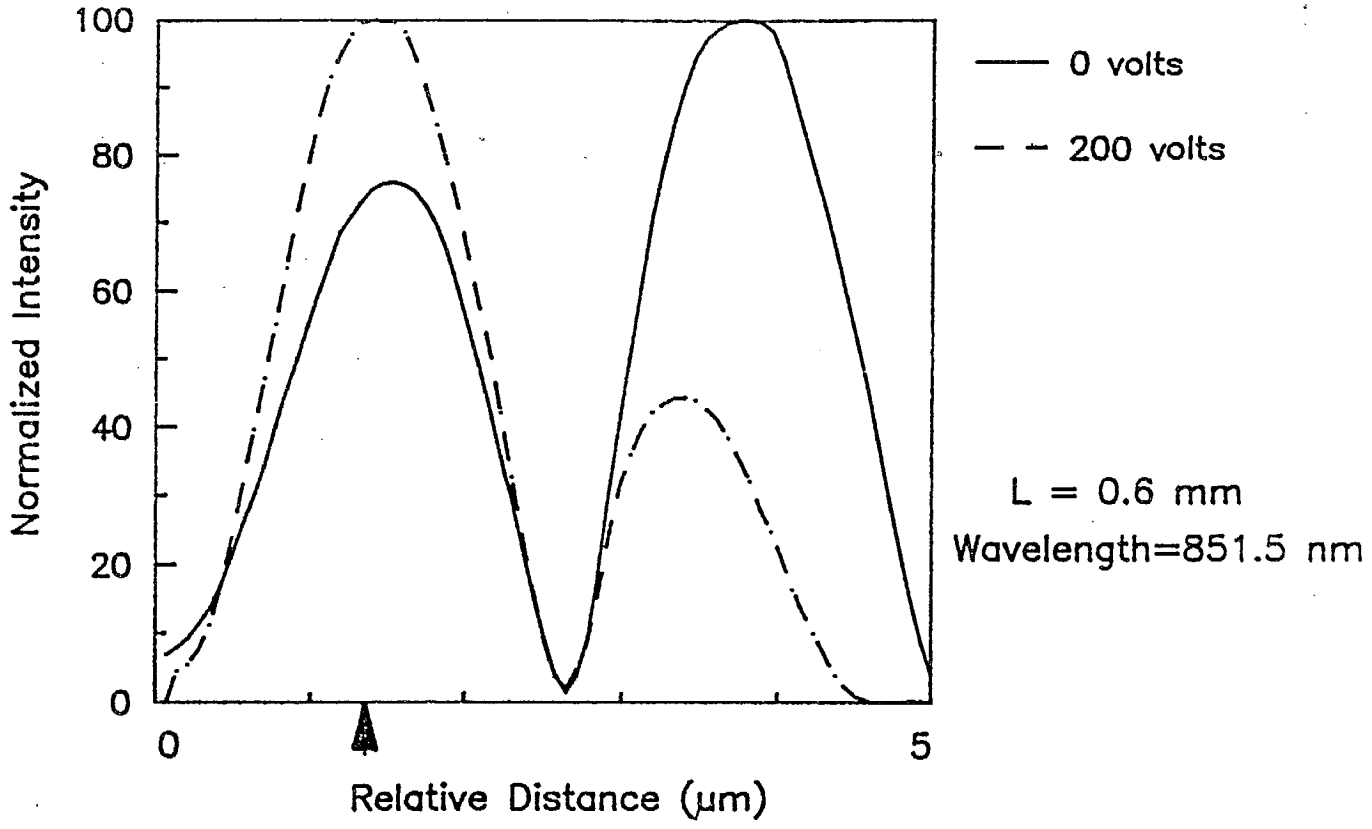

Figure 13. Electrooptic switching - Design #2, L = 0.6 mm.

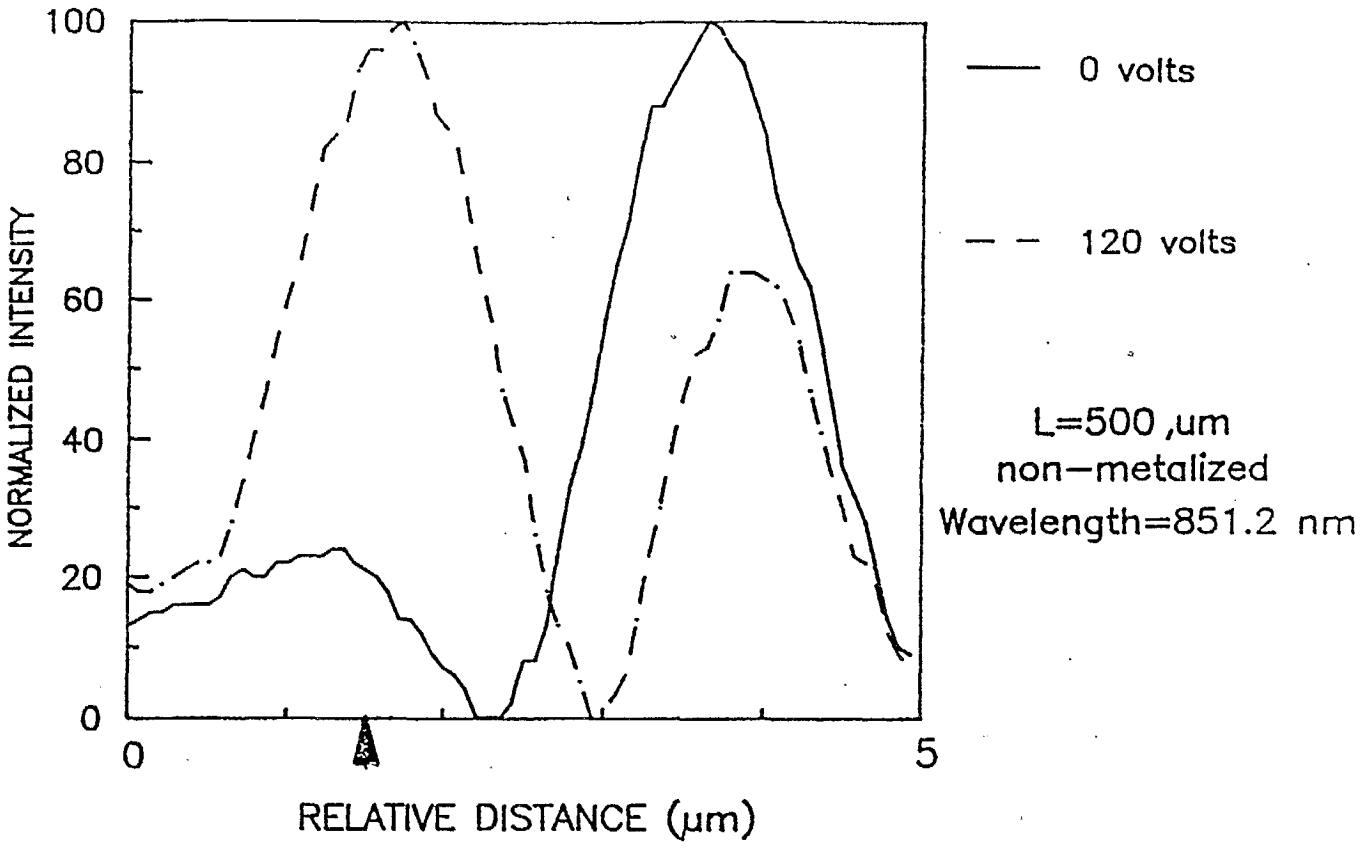

Figure 14. Electrooptic switching - Design #2, L = 0.5 mm.

3.4 V-I Characteristics

When applying a bias potential to each of the samples described above, it was noted that above a certain threshold a current flow would occur as shown in figure 15. While the case presented here is for the 500 μm, non-metalized sample from design 2, the characterics are very similar in each of the other tested cases. We can see that the onset of current flow occurs at an applied bias of 40 volts with the current increasing almost linearly up to 100 volts. Above this point the current begins to level off and becomes virtually constant above 200 volts.

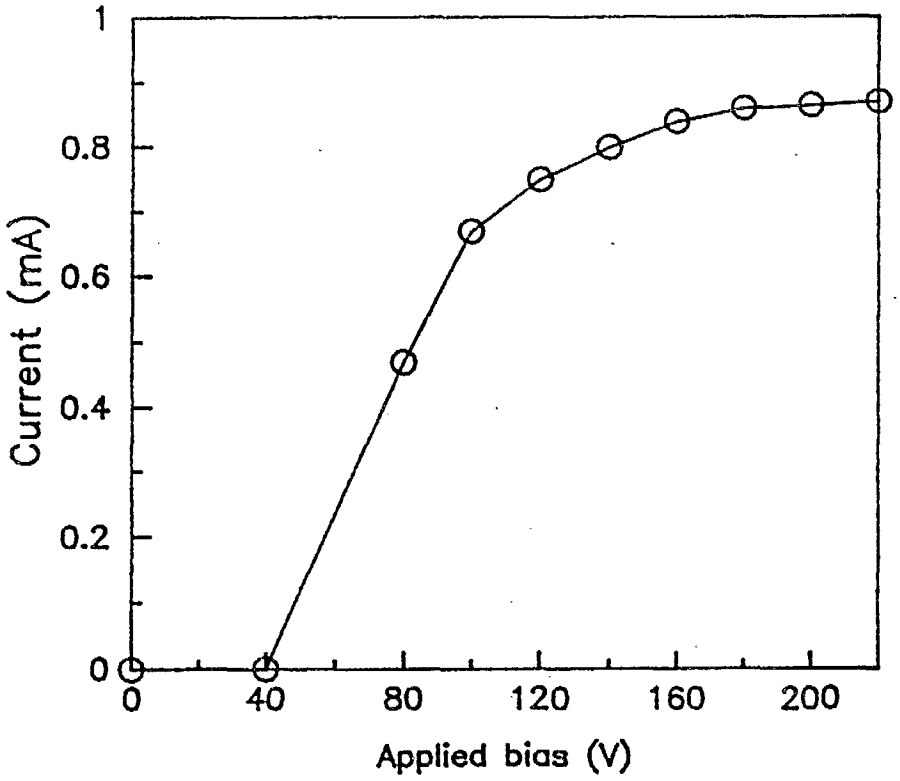

Figure 15. V-I curve for 0.5 mm sample - Design #2.

It is believed that there are at least two sources for this current. The first source may be photoexcited carriers which are swept across the structure by the applied electric field. These carriers may be produced from ionized excitons or may be created directly by high energy photons. This theory was tested by varying the input optical intensity while observing the change in current flow. The results confirmed the presence of a photocurrent but indicated that another mechanism is also involved since the current varied slightly with the optical power but a large percent remained after the optical source was removed.

The second source of current in the structure is believed to be electron-hole pairs which are excited in the semiconductor by the applied electric field. Since the coupler is composed of intrinsic semiconductor materials (i.e. no doping) the electrons are normally in their ground state and the only free carriers are those excited by thermal phonons into conduction. When a large enough electric field is applied, the loosely bound valence electrons are pulled away from the atoms

and become free to contribute to the current flow. The current limiting which occurs at high bias voltages is probably due to band filling which occurs when a large number of electrons are excited into conduction.

The current flow described here is inhibited in most electrooptic device applications by doping the semiconductor layers and forming a p-i-n structure. If a reverse bias is then applied to the device the junctions will prevent any significant current flow other than the photoexcited current from the intrinsic layer. However, it appears that for voltages below 200 volts the current flow does not effect the quantum-confined Stark effect since the shifts in the absorption spectrum reported here match very closely the values achieved in other works.

4. Conclusions

In conclusion, the MQW-coupled nonlinear directional coupler is a highly versatile and promising device for future optical systems. Combination of the effects mentioned above yields a vast number of device configurations which could be implemented with this relatively simple structure. We have concentrated here on the electrooptic switching capabilities of the coupler which are attributed to the quantum-confined Stark effect. The preliminary results demonstrate that electrorefraction in the MQW layer can be used as an efficient switching mechanism. Although the bias voltages required in these experiments were quite high, the field strength in the MQW of approximately 2 V/μm is an attractive result. By doping the substrate and buffer layers to form a p-i-n structure, such a field strength could be achieved with only a few volts of bias. It is this feature along with a high-speed operation potential that makes the MQW-coupled directional coupler, analyzed and tested in this work, a promising realistic candidate for future applications.

The dimensions of the coupler are also quite impressive and are expected to improve in future designs. The samples tested here ranged in length from 406 to 800 μm. A doped version of the first sample design with a gold layer deposited on top is now under development. This design should exhibit very favorable qualities of short coupling length, all-optical switching at low incident powers, and electrooptic

switching with less than 10 volts. The short samples from the first sample design were not tested for electrooptic switching due to the risk of damaging the non-metalized samples.

It is believed that the current flow which was measured while applying a high bias voltage does not interfere with the quantum-confined Stark effect since our estimate of the induced shift in the absorption spectrum is virtually identical to independently measured values. The speed of the device is therefore expected to be limited by the capacitance of the structure which can be reduced by etching away the substrate material. The fundamental limit is then determined by the speed at which the electron wave function can respond or in other words the time required for the electrons and holes to be pulled to opposite sides of the wells. Keeping in mind the uncertainty principle we would expect this response to be limited by the time required for a bound electron to complete one orbit around the exciton. For an exciton diameter of 30 nm the maximum distance travelled is therefore $2\pi r$ = 94.2 nm. Using the saturated drift velocity of a carrier in GaAs when an external field of 1 V/μm is applied, the velocity of the electrons is approximately 10^5 m/sec [33]. This yields a response time limit of 0.94 psec which is in excellent agreement with the predictions of Chemla *et al.* [5].

5. References

[1] "Ultra-high speed solutions", GaAs-ette, published by GigaBit Logic Inc., vol. 3 (2), 1988.

[2] K.Y.Lau, "Semiconductor Sources and Detectors in Fiber-Optic Systems", Microwave Journal, vol. 28 (4), p.97, 1985.

[3] K.Y.Lau, A.Yariv, "Ultra-High Speed Semiconductor Lasers", IEEE J. Quantum Elect., QE-21 (2), p. 121, 1985.

[4] L.Esaki, "A Bird's-Eye View on the Evolution of Semiconductor Superlattices and Quantum Wells", IEEE J. Quantum Electron., vol, QE-22 (9), p.1611, 1986.

[5] D.S.Chemla, D.A.B.Miller, P.W.Smith, "Nonlinear optical properties of GaAs/AlGaAs multiple quantum well material: phenomena and applications", Optical Eng., vol. 24 (4), p.556, 1985.

[6] D.S.Chemla, D.A.B.Miller, P.W.Smith, A.C.Gossard, W.Weigmann, "Room Temperature Excitonic Nonlinear Absorption and Refraction in GaAs/AlGaAs Multiple Quantum Well Structures", IEEE J. Quantum Electron., vol. QE-20 (3), p.265, 1984.

[7] D.A.B.Miller, "Quantum wells for optical information processing", Optical Eng., vol. 26 (5), p.368, 1987.

[8] G.J.Sonek, J.M.Ballentyne, Y.J.Chen, G.M.Carter, S.W.Brown, E.S.Koteles, J.P.Solerno, "Dielectric Properties of GaAs/AlGaAs Multiple Quantum Well Waveguides", IEEE J. Quantum Electron., vol. QE-22 (7), p.1015, 1986.

[9] L.Esaki and R.Tsu, "Superlattice and Negative Conductivity in Semiconductors", IBM Res. Note, RC-2418, Mar. 1969.

[10] S.W.Koch, N.Peyghambarian, H.M.Gibbs, "Band-edge nonlinearities in direct-gap semiconductors and their application to optical bistability and optical computing", J. Appl. Phys., vol. 63 (2), p.R1, 1988.

[11] D.A.B.Miller, J.S.Weiner, D.S.Chemla, "Electric-Field Dependence of Linear Optical Properties in Quantum Well Structures: Waveguide Electroabsorption and Sum Rules", IEEE J. Quantum Electron., vol. QE-22 (9), p.1816, 1986.

[12] M.Whitehead, G.Parry, J.S.Roberts, P.Mistry, P. Li Kam Wa, J.P.R.David, "Quantum-confined Stark shifts in MOVPE-grown GaAs-AlGaAs multiple quantum wells", Electronics Letters, vol. 23 (20), p.1048, 1987.

[13] J.E.Zucker, I.Bar-Joseph, G.Sucha, U.Koren, B.I.Miller, D.S.Chemla, "Electrorefraction in GaInAs/InP Multiple Quantum Well Heterostructures", Electronics Letters, vol. 24 (8), p.458, 1988.

[14] W.H.Knox, D.A.B.Miller, T.C.Damen, D.S.Chemla, C.V.Shank, A.C.Gossard, "Subpicosecond excitonic electroabsorption in room-temperature quantum wells", Appl. Phys. Lett, vol. 48 (13), p.864, 1986.

[15] J.S.Weiner, "Physics and applications of quantum wells in waveguides", SPIE, vol. 578, p.116, 1985.

[16] B.R.Bennett, R.A.Soref, "Electrorefraction and Electroabsorption in InP, GaAs, GaSb, InAs, and InSb", IEEE J. Quantum Electron., vol. QE-23 (12), p.2159, 1987.

[17] D.R.P.Guy, N.Apsley, L.L.Taylor, S.J.Brass, Proc. of SPIE, vol. 792, p.189, 1987.

[18] T.H.Wood, E.C.Carr, C.A.Burrus, J.E.Henry, A.C.Gossard, J.H.English, "High-Speed 2x2 Electrically Driven Spatial Light Modulator Made With GaAs/AlGaAs Multiple Quantum Wells (MQWs)", Electronic Letters, vol. 23 (17), p.816, 1987.

[19] T.H.Wood, C.A.Burrus, R.S.Tucker, J.S.Weiner, D.A.B.Miller, D.S.Chemla, T.C.Damen, A.C.Gossard, W.Weigmann, "100 ps Waveguide Multiple Quantum Well (MQW) Optical Modulator with 10:1 ON/OFF Ratio", Electronic Letters, vol. 21, p.693, 1985.

[20] A.Ajisawa, M.Fujiwara, J.Shimuzu, M.Sugimoto, M. Uchida, Y.Ohta, "Monolithically Integrated Optical Gate 2x2 Matrix Switch Using GaAs/AlGaAs Multiple Quantum Well Structure", Electronics Letters, vol. 23 (21), p.1121, 1987.

[21] Y.Kawamura, K.Wakita, Y.Yoshikuni, Y.Itaya, H.Asahi, "Monolithic Integration of a DFB Laser and an MQW Optical Modulator in the 1.5μm Wavelength Range", IEEE J. Quantum Electron., vol. QE-23 (6), p.915, 1987.

[22] H.Sakaki, H.Kurata, M.Yamanishi, "Novel Quantum-Well Optical Bistabilty Device With Excellent ON/OFF Ratio And High Speed Capability", Electronics Letters, vol. 24 (1), p.1, 1988.

[23] P. Li Kam Wa, J.H.Marsh, P.N.Robson, J.S.Roberts, N.J.Mason, "Nonlinear propagation in GaAs/GaAlAs multiple quantum well waveguides", SPIE, vol. 578, p.110, 1985.

[24] M.Cada, R.C.Gauthier, B.E.Paton, J.Chrostowski, "Nonlinear guided waves coupled nonlinearly in a planar GaAs/GaAlAs multiple quantum well structure", Appl. Phys. Lett., vol. 49 (13), p.755, 1986.

[25] D.A.B.Miller, D.S.Chemla, P.W.Smith, A.C.Gossard, W.Wiegmann, "Nonlinear optics with a diode-laser light source", Optics Letters, vol. 8 (9), p.477, 1983.

[26] S.M.Jensen, "The nonlinear coherent coupler a new optical logic device", presented at Conf. Integrated and Guided-Wave Optics, Incline Village, California, 1980.

[27] M.Cada, B.P.Keyworth, J.M.Glinski, A.J.SpringThorpe, P.Mandeville, "Experiment with multiple-quantum-well waveguide switching element", J. Opt. Soc. Am. B, vol. 5 (2), p.462, 1988.

[28] M.Cada, R.C.Gauthier, J.Chrostowski, B.E.Paton, "Multiple-quantum-well nonlinear coupler", SPIE, vol. 704, p.123, 1986.

[29] M.Cada, R.C.Gauthier, B.E.Paton, J.M.Glinski, "Multiple Quantum Well Coupling Element With Losses", Appl. Phys. Lett., vol. 51 (10), p.713, 1987.

[30] M.Cada, J.D.Begin, R.C.Gauthier, B.E.Paton, "Nonlinear propagation characteristics of optical waveguides involving GaAs-based multiple quantum wells", Proc. of SPIE, vol. 836, p.231, 1987.

[31] B.P.Keyworth, M.Cada, J.M.Glinski, A.J.SpringThorpe, P.Mandeville, "All-Optical Switching in a GaAs-Based MQW Directional Coupler", Canadian J. Physics, vol. 67, p.408, 1989.

[32] M.Cada, B.P.Keyworth, J.M.Glinski, C.Rolland, A.J.SpringThorpe, K.O.Hill, R.A.Soref, "Electro-optical switching in a GaAs multiple quantum well directional coupler", Appl. Phys. Lett., vol. 54 (25), p.2509, 1989.

[33] S.Adachi, "GaAs, AlAs, and $Al_xGa_{1-x}As$: Material parameters for use in research and device applications", J. Appl. Phys., vol. 58 (3), p.R1, 1985.